Allosteric Regulation of Cyclin-B Binding by the Charge State of Catalytic Lysine in CDK1 Is Essential for Cell-Cycle Progression

Shaunak Deota[1], Sivasudhan Rathnachalam[2], Kanojia Namrata[1], Mayank Boob[2], Amit Fulzele[3], RadhikaS.[2], Shubhra Ganguli[4,5], Chinthapalli Balaji[1], Stephanie Kaypee[6], Krishna Kant Vishwakarma[2], Tapas Kumar Kundu[6], Rashna Bhandari[4], Anne Gonzalez de Peredo[3], Mithilesh Mishra[1], Ravindra Venkatramani[2] and Ullas Kolthur-Seetharam[1]

1 - *Department of Biological Sciences,* Tata Institute of Fundamental Research (TIFR), Mumbai 400005, India
2 - *Department of Chemical Sciences,* Tata Institute of Fundamental Research (TIFR), Mumbai 400005, India
3 - *Institut de Pharmacologie et de Biologie Structurale (IPBS),* Toulouse 31400, France
4 - *Laboratory of Cell Signalling,* Centre for DNA Fingerprinting and Diagnostics (CDFD), Hyderabad 500039, India
5 - *Graduate Studies,* Manipal Academy of Higher Education, Manipal 576104, India
6 - *Transcription and Disease Laboratory,* Molecular Biology and Genetics Unit, Jawaharlal Nehru Centre for Advanced Scientific Research (JNCASR), Bengaluru 560064, India.

Correspondence to Ravindra Venkatramani and Ullas Kolthur-Seetharam: *ravi.venkatramani@tifr.res.in,* *ullas@tifr.res.in*
https://doi.org/10.1016/j.jmb.2019.04.005
Edited by Richard W. Kriwacki

Abstract

Cyclin-dependent kinase 1 (CDK1) is essential for cell-cycle progression. While dependence of CDK activity on cyclin levels is well established, molecular mechanisms that regulate their binding are less understood. Here, we report for the first time that CDK1:cyclin-B binding is not default but rather determined by the evolutionarily conserved catalytic residue, lysine-33 in CDK1. We demonstrate that the charge state of this lysine allosterically remodels the CDK1:cyclin-B interface. Cell cycle-dependent acetylation of lysine-33 or its mutation to glutamine, which mimics acetylation, abrogates cyclin-B binding. Using biochemical approaches and atomistic molecular dynamics simulations, we have uncovered both short-range and long-range effects of perturbing the charged state of the catalytic lysine, which lead to inhibition of kinase activity. Specifically, although loss of the charge state of catalytic lysine did not impact ATP binding significantly, it altered its orientation in the active site. In addition, the catalytic lysine also acts as an intra-molecular electrostatic tether at the active site to orient structural elements interfacing with cyclin-B. Physiologically, opposing activities of SIRT1 and P300 regulate acetylation and thus control the charge state of lysine-33. Importantly, cells expressing acetylation mimic mutant of Cdc2/CDK1 in yeast are arrested in G2 and fail to divide, indicating the requirement of the deacetylated state of the catalytic lysine for cell division. Thus, by illustrating the molecular role of the catalytic lysine and cell cycle-dependent deacetylation as a determinant of CDK1:cyclin-B interaction, our results redefine the current model of CDK1 activation and cell-cycle progression.

© 2019 Elsevier Ltd. All rights reserved.

Introduction

Cyclin-dependent kinases (CDKs) are evolutionarily conserved protein kinases, which play key roles in eukaryotic cell division cycles, differentiation and transcription [1,2]. Among these, CDK1 (or yeast Cdc2 and Cdc28), CDK2, CDK4 and CDK6 orchestrate cell-cycle progression. As CDKs are constitutively expressed, binding to cyclins that have cell-cycle phase-dependent expressions is essential for CDK activation [1]. Our current understanding of the temporal control of CDK activity is based on the

inhibitory and activatory phosphorylations, brought about by a regulatory loop involving other kinases and phosphatases [3].

Several reports have investigated structural determinants and the impact of phosphorylations in stabilizing either the inactive or active kinase conformations [4–6]. Uniquely in CDKs, and unlike in other kinases, binding of cyclin induces the movement of PSTAIRE-/C-helix to bring together a set of catalytic triad residues (lysine, aspartate and glutamate), which are otherwise far apart in apo-CDKs to form a competent kinase active site [5,7]. Given the essentiality of cyclin binding for CDK activation and hence cell-cycle progression, physiologically relevant molecular mechanisms that determine complex formation remain to be addressed. Specifically, deterministic residues within CDKs that may regulate cyclin binding/unbinding, and therefore contributing to cell division, have not been explored. It is important to emphasize that the binding of cyclins to CDKs has been generally thought to be default in the field.

Eukaryotic protein kinases (EPKs), including CDKs, have been reported to be acetylated [8–14]. CDK2, CDK5 and CDK9 are acetylated at their catalytic lysine and acetyl-mimic mutations (lysine to glutamine) led to a complete loss of kinase activity [9–11,15,16]. However, none of these studies have provided insights on the molecular mechanisms by which lysine acetylation led to a loss in protein function. Specifically, if and how acetylation-dependent masking of the positive charge on the catalytic lysine impacts the CDK–cyclin complex remains unknown.

Here, we have investigated the importance of acetylation and hence the charge state of catalytic lysine-33 in CDK1/Cdc2 in regulating its functions. CDK1 (Cdc28 or Cdc2 in yeast) is an essential kinase for G2-M transition and mitosis, whose structure in complex with cyclin-B was only recently resolved [17]. We show for the first time that perturbing the charge state of catalytic lysine allosterically impairs the ability of CDK1 to bind with cyclin-B, which is generally thought to be default. In addition to illustrating that lysine-33 acetylation is dynamically regulated across the cell cycle, we clearly demonstrate that mutation to acetyl-mimic glutamine in Cdc2 affects cell-cycle progression and survival. Taken together, this study identifies the charge state of catalytic lysine to play a pivotal role in cyclin-B binding and deacetylation as a novel regulatory mechanism for activation of CDK1.

Results

SIRT1 and P300 regulate acetylation of the conserved catalytic lysine in CDK1

Given that CDKs are acetylated, if and how acetylation impinges on their structural and functional states is poorly understood. Specifically, the impact of lysine acetylation on CDK1 function, which in general cannot be compensated by any of the other CDKs [18], has not been addressed thus far. In this context, we probed CDK1 acetylation in mammalian cells, and indeed found immunoprecipitated CDK1-HA to be acetylated (Fig. 1a). Based on our global LC–MS/MS analyses of the acetylated sub-proteome, we mapped lysine-33 as the sole acetylation site in endogenous CDK1 (Fig. 1b), as reported earlier [8]. To further characterize the importance of this acetylation, we generated antibodies specific to the lysine-33 acetylated peptide sequence ^{30}VAM**K**^{Ac}KIRLESE^{40} in CDK1 (α-CDK1-K33Ac/α-K33Ac). This region is largely conserved across CDKs and specifically in CDK1 from yeast to humans (Fig. S1a–c). Immuno-affinity-purified α-K33Ac antibodies were able to detect endogenous CDK1 acetylation at lysine-33 (Fig. 1c) and did not react with CDK1-K33R mutant (Fig. S1d). Furthermore, we could detect acetylated species of CDK1 using both pan-acetyl-lysine and α-K33Ac antibodies (Fig. 1c). These clearly corroborated the LC–MS/MS results vis-à-vis acetylation of CDK1 at lysine-33.

Protein acetylation is regulated by activities of lysine acetyltransferases (KATs) and lysine deacetylases (KDACs). Hence, to identify the acetyltransferase responsible for acetylating CDK1 at lysine-33, we expressed CDK1-HA along with KATs: P300, PCAF and GCN5. As can be seen from Fig. 1d, CDK1-acetylation was significantly enhanced in response to P300 expression when compared to PCAF and GCN5. Moreover, P300 was able to acetylate CDK1 *in vitro* (Fig. S1e). These results are consistent with earlier reports showing CDK1–P300 interaction and CDK1-mediated phosphorylation of P300 [19].

To identify the KDAC, we treated cells with nicotinamide (NAM) and Trichostatin A, which non-overlappingly inhibit sirtuins (NAD$^+$-dependent deacylases) and non-sirtuin KDACs, respectively. We found that there was a robust increase in CDK1 acetylation following NAM treatment, clearly indicating an involvement of sirtuins (Fig. 1e). Moreover, CDK1 and SIRT1 have been shown to interact with each other ([20] and Fig. S1f), although the biological relevance of this interaction has not been investigated. Given this, we indeed observe that SIRT1 overexpression led to a reduction in CDK1 acetylation (Fig. 1f and g). Taken together, these results clearly illustrate that P300 is the major KAT for CDK1 at lysine-33 and that SIRT1 is involved in its deacetylation.

Acetylation of CDK1 at lysine-33 impairs its kinase activity

Evolutionarily conserved lysine-33 lies in the catalytic pocket of CDK1 where ATP binds, and analogous
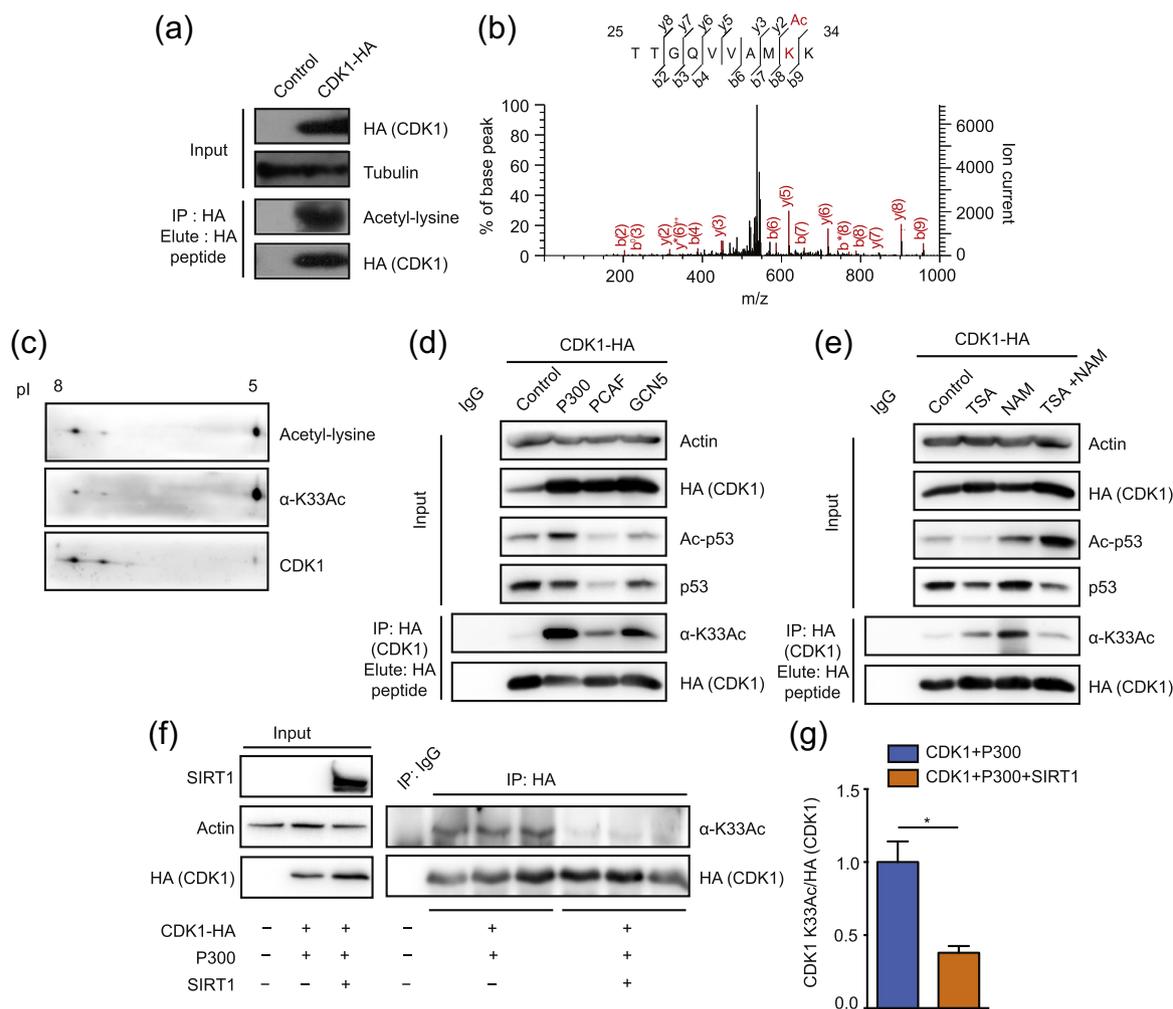
Fig. 1. *In vivo* CDK1 acetylation at lysine-33 is regulated by opposing actions of P300 and SIRT1. (a) Immunoprecipitated CDK1-HA was probed with α-pan-acetyl lysine antibody to reveal acetylation. (b) Identification of lysine-33 as the site of acetylation in CDK1 by LC–MS/MS analysis. (c) 2D-PAGE of immunoprecipitated endogenous CDK1 from HEK 293T cells and immunoblot with α-pan-acetyl-lysine or α-CDK1-K33Ac antibodies confirms acetylation. (d–e) Probing for acetylation of immunoprecipitated CDK1-HA from cells (d) co-transfected with P300, PCAF or GCN5, shows P300 as the major KAT and (e) treated with KDAC inhibitors indicates NAM-sensitive acetylation. (f–g) Probing for acetylation of immunoprecipitated CDK1-HA from cells co-transfected with P300 or P300/SIRT1 shows SIRT1 mediated attenuation of P300-dependent CDK1 lysine-33 acetylation. Representative immunoblot (f) and quantification of pixel intensities (g) from panel f. Error bars represent SEM for n = 3 technical replicates from a representative experiment.

active-site lysines in other CDKs and in fact all other kinases have been implicated in kinase activity [9–12,16,21–28]. Hence, to check the importance of lysine-33 acetylation for CDK1 function, we employed K33R and K33Q mutants of CDK1, which have typically been used as deacetylation and acetylation mimics, respectively. *In vitro* kinase assays of CDK1-WT and -K33Q, immunoprecipitated from G2/M synchronized cells co-expressing cyclin-B1 (Fig. S2b), showed that K33Q mutation completely abrogated the CDK1 activity (Fig. 2a and b). Incubating CDK1:cyclin-B with P300 and acetyl-CoA led to acetylation of CDK1 *in vitro*, and this resulted in reduced kinase activity (Fig. S2e–g). The decrease

was small, which is possibly due to only a minor fraction of CDK1 being acetylated by P300 under the conditions of the assay. However, as with other acetylated proteins, it is difficult to draw a direct correlation between stoichiometry of acetylation and enzymatic activity particularly when assaying a mixed pool of acetylated and un-acetylated proteins, as would be the case *in vivo*. This nevertheless indicated that P300 could acetylate CDK1 in complex with cyclin-B and raises the possibility of acetylation-dependent dissociation of cyclin-B, possibly post-metaphase during mitosis. Future studies would likely reveal if this acts as a regulatory modification that ultimately leads to cyclin-B degradation. Interestingly,

CDK1-K33R also abolished kinase activity despite retaining the charge state (Fig. S2a), as with other kinases with similar arginine substitutions [12,23–28]. It is important to note that although mutations of the catalytic lysine have been shown to abolish CDK activity, the underlying molecular mechanism is still unknown [9–11,15,16,22]. Notably, these results indicated that both the lysine side-chain and its charge state are essential determinants of kinase activity.

Mutations of tyrosine-15 and threonine-161 (inhibitory and activatory phosphorylation sites, respectively) or aspartate-146 (in DFG motif) in CDK1 affect cell-cycle progression [21,29–33]. Unlike these mutants, overexpression of CDK1-K33Q did not lead to a dominant negative phenotype (Figs. S2c and d). Possibly owing to the kinase dead CDK1-K33Q mutant, we could not generate a cell culture system to assay for the acetyl-mimic mutant in a background wherein the endogenous wild-type CDK1 was absent. In this context, it is important to note that mutating an orthologous lysine residue to the acetyl-mimic glutamine (K40Q) in Cdc28 results in lethality [8]. Therefore,

we resorted to using ectopically expressed CDK1-K33Q mutant to dissect out the molecular mechanism of loss of kinase activity.

Inhibitory phosphorylation at tyrosine-15 prevents precocious activation and is an indicator of inactive CDK1. Upon assaying for phospho-tyrosine-15, we did not find any significant difference between CDK1-WT and -K33Q (Fig. 2c and d). This clearly rules out inhibitory phosphorylation as causal for inactivation of CDK1-K33Q mutant. Along with comparable levels of expressed wild-type and mutant CDK1, similar extents of inhibitory phosphorylation indicate that the mutations do not lead to destabilization of the protein. Moreover, this motivated us to investigate a hitherto unknown mechanism of CDK1 activity regulation that is dependent on the catalytic lysine residue.

Modeling and simulations of WT, K33Q and K33Ac CDK1:cyclin-B:ATP complexes

Next, we investigated how lysine-33, its acetylation or the mutation to acetyl-mimic glutamine affected
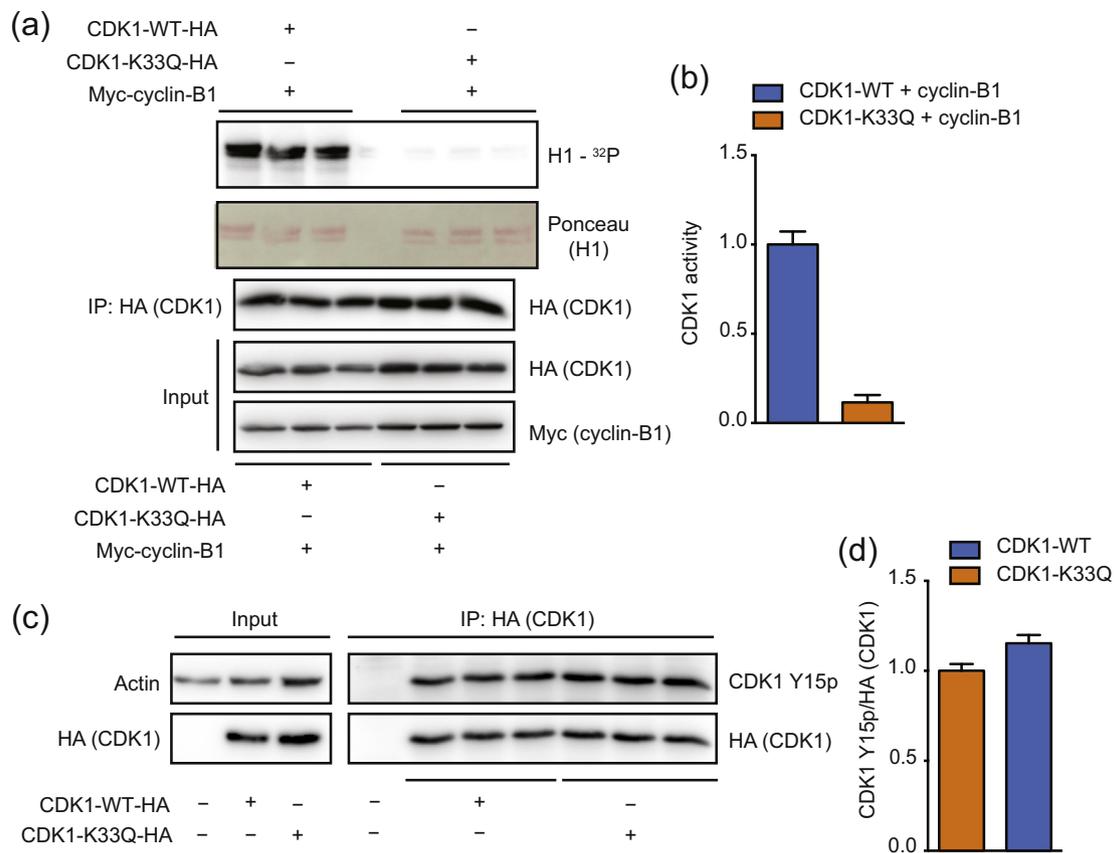
Fig. 2. CDK1 acetylation at lysine-33 inhibits kinase activity. (a–b) H1 phosphorylation by CDK1-K33Q expressed relative to the activity of CDK1-WT shows lysine-33 mutation abrogates kinase activity. Error bars represent SEM for n = 3 technical replicates for two experimental repeats. (c–d) Immunoprecipitated CDK1-WT-HA or -K33Q-HA probed with α-phospho-tyrosine-15 CDK1 (CDK1 Y15p) antibodies reveals no change in inhibitory CDK1-Y15 phosphorylation. Error bars represent SEM for n = 3 technical replicates from a representative experiment.

CDK1:cyclin-B:ATP active complex, through modeling and computational analyses. To this end, we used the PDB ID: 4Y72 complex [17] and docked an ATP molecule into the catalytic pocket. Given that a very recent study reported structures for other inhibitor bound complexes [34], we compared these with the 4Y72 complex and found them to be nearly overlapping (Fig. S3a–b). We generated the wild-type CDK1:cyclin-B:ATP ternary complex model and validated it using the ATP bound CDK2:cyclin-A crystal structure (Fig. 3a), given their active site structural similarities. We also generated models for CDK1-K33Q and CDK1-K33Ac (lysine-33 replaced with acetyl-lysine) (Supplementary table S1). We would like to point out that the initial binding mode of ATP for all three models was the same. The
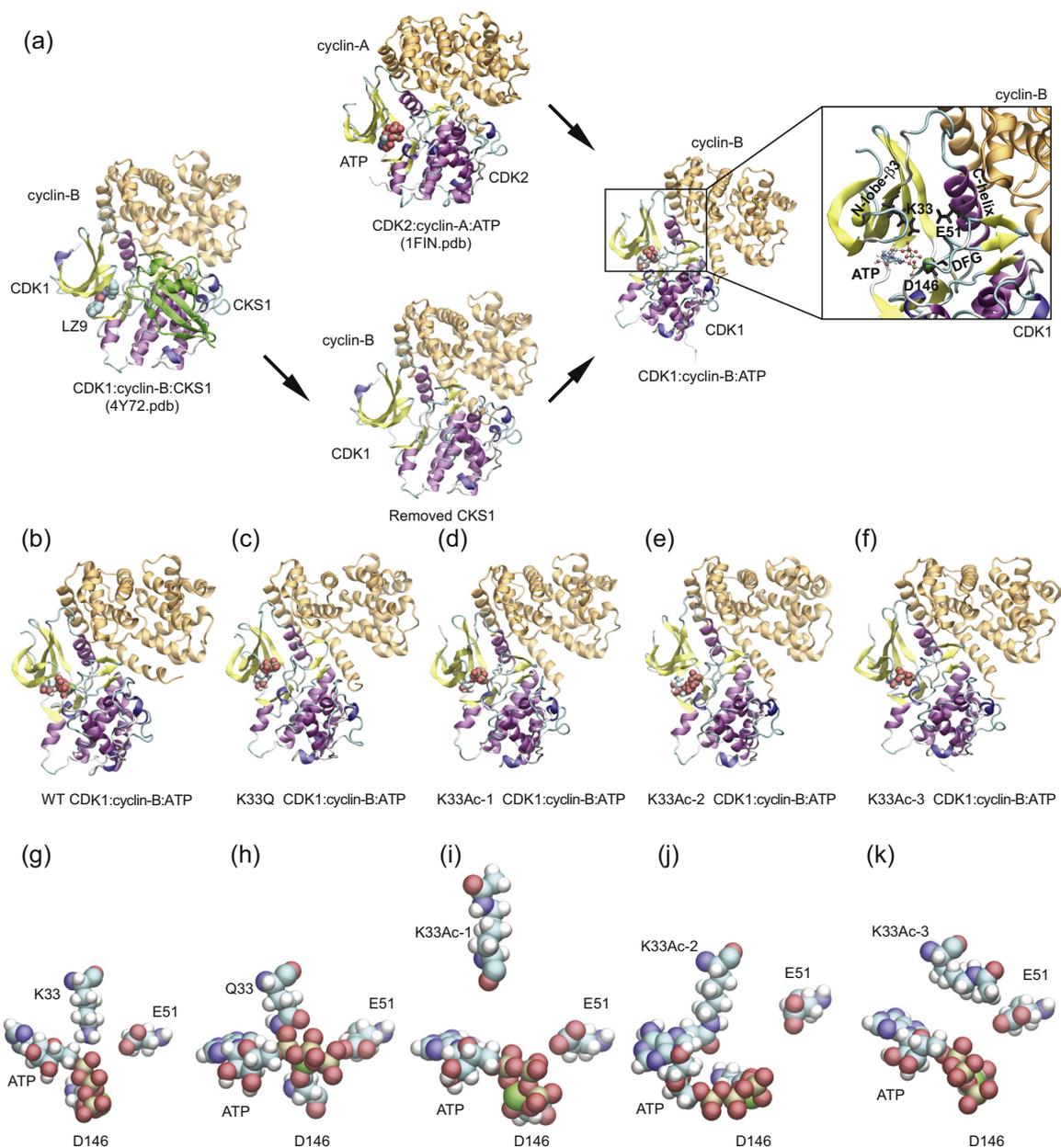
Fig. 3. CMD simulations for WT, K33Q and K33Ac-1,-2,-3 CDK1:cyclin-B:ATP ternary complexes. (a) Workflow depicting modeling of WT, K33Q and K33Ac-1,-2,-3 CDK1:cyclin-B:ATP ternary complexes. (b–k) Structures for WT, K33Q and K33Ac-1,-2,-3 CDK1:cyclin-B:ATP ternary complexes obtained from 200-ns NVT CMD simulations. (b–f) show CDK1 (multi-color) and cyclin-B (orange) in secondary structure representation and ATP bound at the CDK1 active site is shown in atomic van der Waals spheres representation. (g–k) View of the active site showing key catalytic triad residues: lysine-33 (K33)/glutamine-33 (Q33)/acetyl-lysine (K33Ac), glutamate-51 (E51) and aspartate-146 (D146) interacting with the bound ATP and Mg^{2+} (green).

atomistically detailed models were solvated, equilibrated at standard temperature (300 K) and pressure (1 bar), and subjected to 200-ns classical molecular dynamics (CMD) simulations to relax the complexes to their native ternary form. Importantly, given that acetylated lysine is bulkier than lysine (Fig. S3c), we employed three different equilibration protocols to study the impact of K33Ac on CDK1:cyclin-B:ATP complex. Specifically, we obtained three distinct structurally relaxed conformations of the ternary complex after equilibration: CDK1-K33Ac-1 (ATP, E51 both constrained during equilibration), CDK1-K33Ac-2 (ATP unconstrained, E51 constrained during equilibration), and CDK1-K33Ac-3 (ATP constrained, E51 unconstrained during equilibration) (Fig. 3b–f and Fig. S3d–h). We stress that no constraints were employed in the 200-ns production simulations. In the case of CDK1-K33Ac-1, but not in others, the acetyl-lysine residue flipped out of the active-site pocket during production runs. In CDK1-K33Ac-2 and -K33A-3, the uncharged residue was observed to interact with the ATP nucleobase (Fig. 3g–k and Fig. S3i–m).

Catalytic lysine in CDK1 plays distinct roles in stabilizing ATP and influencing interactions with cyclin-B

We examined, *in silico*, the effect of lysine-33 perturbations on ATP binding in terms of the following two measures: (a) Solvent accessibility of ATP in the catalytic pocket relative to its accessibility in free solution (relative SASA), and (b) non-bonded (electrostatic and van der Waals) interaction energy of ATP with residues in the catalytic pocket (Fig. 4b). As shown in Fig. 4a, more than 60% of the ATP surface area is buried in the active site in all five complexes (CDK1-WT, -K33Q, and the three -K33Ac models). Although in the CDK1-K33Ac-2 model, we observed transient fluctuations in the relative SASA for ATP during the 200-ns MD trajectory, the averaged values over the entire timescale show that ATP is buried in the active site as in the other models. Nevertheless, we found that with the loss of electrostatic interactions of ATP tail with lysine-33, as in CDK1-K33Q and -K33Ac complexes, the conformation adopted by ATP was different when compared to CDK1-WT (Fig. 4d). We further assessed the non-bonded interaction energy (E_{NB}) of ATP with residues of the active-site pocket within a 3- to 7-Å radius around the ATP. In the wild-type complex, for residues within 3 Å, E_{NB} was close to -400 kcal/mol and become slightly more favorable (to around -450 kcal/mol) when residues up to 5 Å were included (Figs. 4b and S3n). In CDK1-K33Q and -K33Ac complexes, the ATP E_{NB} values were comparable to each other but less favorable (by about 100–200 kcal/mol), vis-à-vis CDK1-WT for interactions with residues within a 3- to 7-Å radius. Moreover, our analyses

clearly suggested that interactions of ATP with residues beyond 5 Å appear to be insignificant, leading to negligible changes in E_{NB} for both CDK1-WT and mutant complexes.

An analysis of ATP interactions with the core catalytic triad (residue-33, aspartate-146, and glutamate-51) showed that lysine-33 was one of the major contributors in terms of binding energetics (Fig. 4c). However, it should be noted that despite the loss of favorable non-bonded interactions, as in the case of CDK1-K33Q and -K33Ac, the overall interactions ($E_{NB} < -200$ kcal/mol) of ATP with the residues of active-site pocket remain highly favorable (Fig. 4b). In summary, ATP appears to be stably bound, albeit with different binding modes in CDK1-WT, -K33Q and -K33Ac complexes. In particular, we find that the Mg^{2+} coordination sphere, which includes oxygens of ATP, acidic residues at the active site and water molecules to be different for CDK1-WT, -K33Q and -K33Ac complexes (Fig. 4d). Based on these results on lysine-33 perturbations in CDK1 and the previous report of lysine-72 mutations in PKA [28], we propose that the catalytic lysine may be dispensable for stable ATP binding in EPKs. Nevertheless, our analyses raise the possibility of lysine-33 playing a key role in the phosphoryl-transfer reaction, which needs to be addressed in the future.

Interactions between the catalytic residues lysine and glutamate on N-lobe-β3 and C-helix, respectively, have been proposed to be important for kinase activity in almost all EPKs [35,36]. Specifically in CDKs, cyclin binding induces a salt-bridge interaction between the catalytic lysine and PSTAIRE-/C-helix glutamate [6,17,37]. Importantly for CDKs, the impact of the loss of lysine charge state on salt bridge with glutamate and PSTAIRE-/C-helix interactions has not been investigated. In this regard, for CDK1-WT, we found that lysine-33 interacted with both glutamate-51 and ATP during the time course of the simulations, showing more prominent interactions with the latter (Fig. S3o–q). The change in the lysine-33 charge state caused a small rotation of the PSTAIRE-helix axis by ~5° in the CDK1:cyclin-B interfacial plane (Fig. S4a and b), and also changed the position and conformation of the T-loop (activation segment) in the CDK1 catalytic domain (Fig. S4c and d). However, we did not find any movement of either the PSTAIRE-/C-helix or glutamate-51 toward the ATP because of the loss of lysine-33 charge state (Fig. S3r–t), unlike what was recently reported for PKA [28]. This indicates that the catalytic lysine, while being indispensable, plays differential roles in rendering kinases active across EPKs.

Mutational analyses and structural evidences have indicated that PSTAIRE-/C-helix in CDK1 is involved in binding to cyclin-B, similar to CDK2:cyclin-A [5,6,17,38]. However, the forces/interactions that stabilize the CDK:cyclin complex remain unclear. In
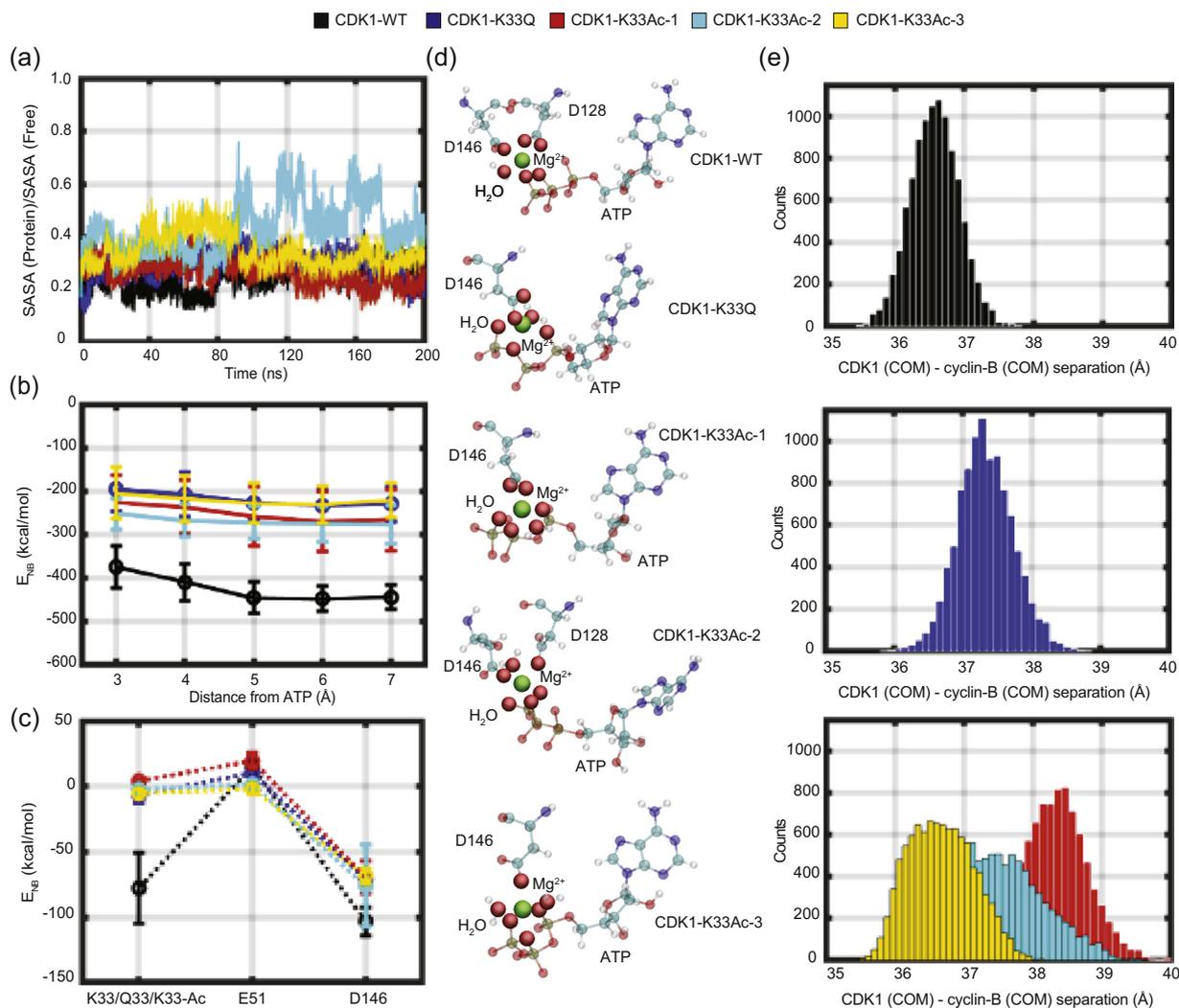
Fig. 4. Loss of CDK1 lysine-33 charge state impinges on active site ATP conformation and weakens CDK1:cyclin-B complexation. (a) Fractional solvent accessible surface areas (SASA) for ATP (ratio of values in ternary complex and free solution) obtained during 200-ns NVT CMD trajectories for WT, K33Q and K33Ac CDK1:cyclin-B:ATP systems are compared. (b) Comparison of non-bonded interaction energies (E_{NB}) of ATP with surrounding active-site residues within a 3- to 7-Å radius in WT, K33Q and K33Ac CDK1:cyclin-B:ATP systems. Error bars represent SD. (c) A comparison of non-bonded interaction energy (E_{NB}) of ATP with catalytic triad residues, residue-33 (K33, Q33, K33Ac), aspartate-146 (D146), and glutamate-51 (E51) in WT, K33Q and K33Ac CDK1:cyclin-B:ATP systems highlights significant contributions from K33, which are reduced upon mutation. Error bars represent SD. (d) ATP orientations and Mg^{2+} (green) coordination spheres (including solvation) in WT, K33Q and K33Ac CDK1:cyclin-B:ATP complexes. The ATP active-site conformation and Mg^{2+} coordination are altered upon mutating lysine-33. (e) Histograms of COM distances between CDK1 and cyclin-B reveal greater separations and broader distributions of distances in K33Q and K33Ac CDK1:cyclin-B:ATP complexes relative to WT.

our attempts to examine the consequences of loss of lysine-33 charge state, we discovered a striking change in the distribution of center-of-mass (COM) distances between CDK1 and cyclin-B proteins in the CDK1-K33Q and -K33Ac complexes relative to the CDK1-WT. As can be clearly seen in Fig. 4e, the distribution of CDK1:cyclin-B COM separations for the mutant lysine-33 complexes (CDK1-K33Q, -K33Ac-1 and -K33Ac-2) distinctly shift to larger values relative to CDK1-WT. For CDK1-K33Ac-3,

while there is no significant shift in peak COM values, the distribution broadens significantly, indicating higher flexibility in the binding geometry of the two proteins. In fact, the widths of distribution of the inter-protein separations along our MD trajectories are the smallest for CDK1-WT. These observations suggest that the perturbations of lysine-33 could be involved in remodeling the CDK1:cyclin-B interface, which was unknown thus far. Furthermore, since the lysine is an active-site residue, far removed from

the CDK1:cyclin-B interface (Fig. 3a), its influence in remodeling the protein–protein interface is allosteric in nature.

To summarize, our *in silico* structural analyses using multiple CDK1:cyclin-B:ATP ternary complexes led us to hypothesize that (a) while the charge state of lysine-33 in the catalytic pocket was necessary for orienting ATP, it may be dispensable for its binding, and (b) perturbing lysine-33 could allosterically influence CDK1 interactions with cyclin-B. We therefore
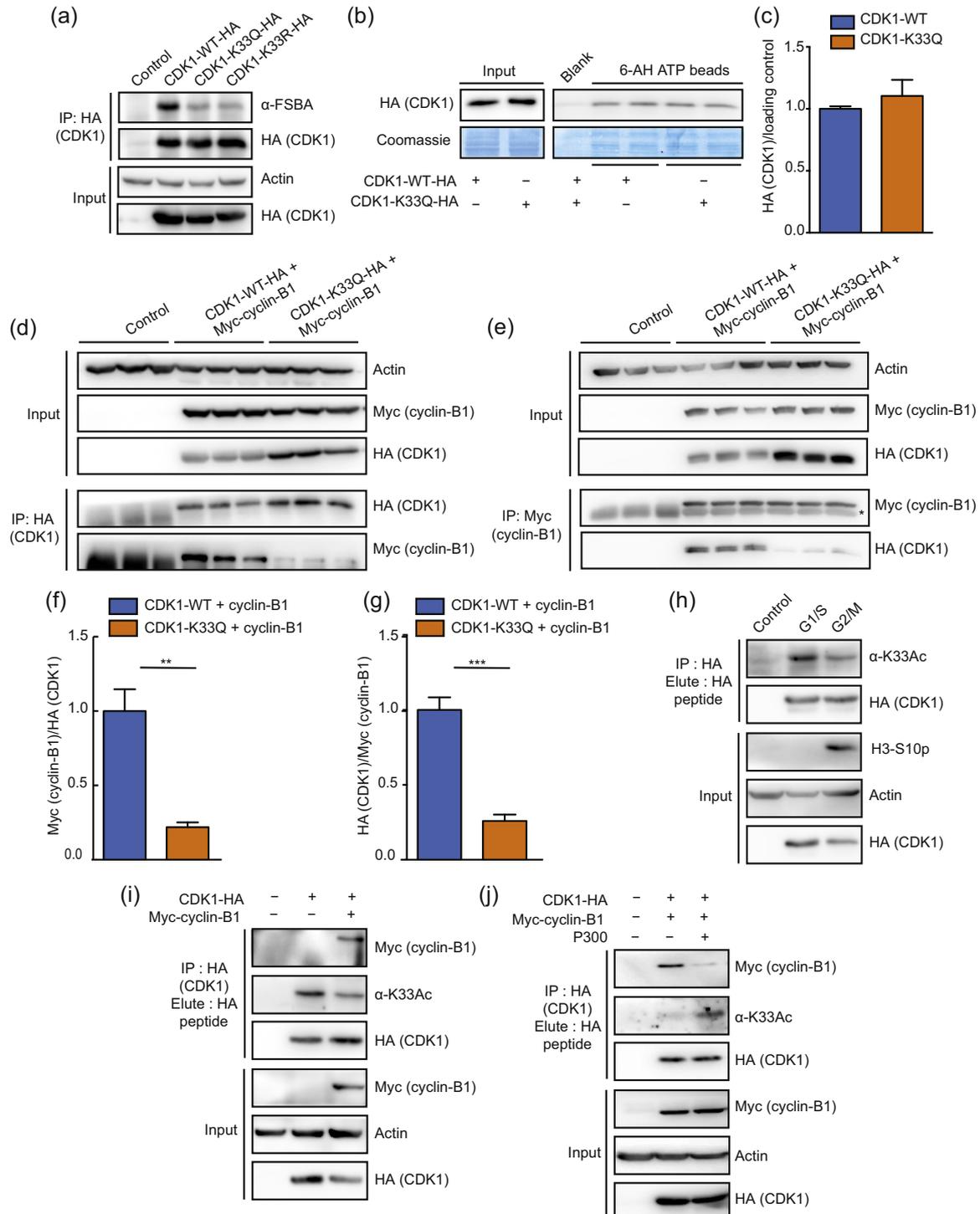

Fig. 5 (*legend on next page*)

set out to validate these hypotheses using biochemical approaches.

Catalytic lysine-33 is dispensable for ATP binding

To check if lysine-33 is required for ATP binding, we used the following approaches: (a) binding of 5′-(4-fluoro-sulfonyl-benzoyl)-adenosine (FSBA), an analog of ATP and (b) ATP-agarose in which ATP is conjugated to the beads in different orientations. Consistent with previous reports from CDK9 [9] and Cdc2 [39], CDK1-K33Q and -K33R mutants had reduced FSBA binding (Fig. 5a). FSBA covalently binds to the active-site lysine with high affinity [40]. Moreover, unlike FSBA, ATP is non-covalently coordinated in the catalytic pocket. Thus, FSBA binding that is equivalently affected in CDK1-K33Q and -K33R does not reveal the importance of lysine in ATP binding.

We found that CDK1-WT bound 6-AH ATP-beads (ATP conjugation *via* C6 of adenine base with a linker) better than the others and were used for further analyses (Fig. S5a). Next, we assessed the relative binding efficiency of CDK1-WT, -K33Q and -K33R to the ATP-conjugated beads. In contrast to our results with FSBA, we found that steady-state ATP binding is not affected by these mutations in CDK1 (Fig. 5b and c and Fig. S5b and). Nevertheless, in binding competition assays using ATP in solution, we found small differences between CDK1-WT, -K33Q and -K33R (Fig. S5d and e). These results clearly indicate that the catalytic pocket lysine or its charge state is dispensable for steady-state ATP binding and importantly corroborate our predictions based on the *in silico* analyses.

Non-default binding of cyclin-B to CDK1 is determined by the charge state of catalytic lysine

Having ruled out all known possible mechanisms that led to CDK1 inactivation due to the alterations of catalytic lysine and motivated by our *in silico* results, we wondered if cyclin-B binding itself is affected. To test this, we probed for the interaction of CDK1-WT, -K33Q and -K33R with cyclin-B1 by reversible co-immunoprecipitations. Remarkably, we found that CDK1-K33Q, which takes away the lysine-33 charge and is typically used as an acetylation mimic, showed reduced interaction with cyclin-B1 (Fig. 5d–g). On the contrary, CDK1-K33R, which retains the lysine-33 charge state and mimics constitutively deacetylated state, remained bound to cyclin-B1 (Fig. S5f and g).

Given that we found endogenous CDK1 lysine-33 to be acetylated, which would naturally mask its charge state, we wanted to assess if acetylation is a determinant of cyclin-B binding in a cell cycle-dependent manner. Despite our best attempts, we could not map differential acetylation of endogenous CDK1 during different phases of cell cycle using α-K33Ac antibodies. As is known for most posttranslational modifications, including key regulatory phosphorylations [41,42], stoichiometry of protein acetylation has been shown to be relatively low [43–45]. Therefore, our inability to quantitatively estimate cell cycle-dependent changes in acetylation could be due to low abundance of acetylated CDK1 combined with the low sensitivity of α-K33Ac antibodies. Nevertheless, using over-expressed CDK1, we investigated if the acetylation and deacetylation potential was indeed regulated in a cell cycle-dependent manner. As shown clearly in Fig. 5h and h, we found hypoacetylated CDK1 in G2/M synchronized cells when compared to cells arrested in G1/S. Importantly, overexpression of cyclin-B1, which increases G2/M population, also resulted in reduced CDK1 lysine-33 acetylation (Fig. 5i). This was consistent with our hypothesis of deacetylation of catalytic lysine as a determinant of cyclin-B binding. We further assayed for CDK1:cyclin-B1 complexes under conditions, which led to increased CDK1 lysine-33 acetylation, by immunoprecipitation. As anticipated, we found that hyperacetylated CDK1 showed significantly less cyclin-B1 association (Fig. 5j). Together, we have found CDK1:cyclin-B interaction to be regulated, which was hitherto unknown. Importantly, our findings establish that

Fig. 5. CDK1 acetylation at lysine-33 does not affect ATP binding but reduces cyclin-B1 interaction. (a) Probing FSBA-labeled CDK1-WT/-K33Q/-K33R-HA immunoprecipitates with α-FSBA antibodies revealed reduced binding upon K33 mutation. (b) Probing for CDK1-WT-HA and -K33Q-HA binding (pull-down) by ATP-conjugated agarose beads (6-AH beads having ATP conjugation *via* C6 of adenine base with a linker) shows no change in steady-state binding. Coomassie staining of total bound proteins was used for normalization. (c) Quantification of ATP binding in panel b. Error bars represent SEM for n = 5 technical replicates from two experimental repeats. (d–g) Reversible co-immunoprecipitations of CDK1-WT-HA or -K33Q-HA and Myc-cyclin-B1 shows reduced CDK1:cyclin-B1 binding upon K33Q mutation. Immunoprecipitation of complexes with α-HA (d) and α-Myc antibodies (e). (f and g) Quantifications of results presented in panels d and e, respectively. *Marks the IgG heavy chain. Error bars represent SEM for n = 3 technical replicates from a representative experiment. (h) Probing for acetylation in immunoprecipitated CDK1-HA shows reduced CDK1 lysine-33 acetylation in G2/M-synchronized cells as compared to G1/S phase. Phospho-H3 S10 (H3-S10p) was used as a marker for G2/M population. (i) Immunoprecipitated CDK1-HA shows negative correlation between CDK1 lysine-33 acetylation and CDK1:cyclin-B1 complexation on probing with α-K33Ac and α-Myc antibodies. (j) Probing immunoprecipitated CDK1-HA with α-K33Ac and α-Myc antibodies from cells transfected with Myc-cyclin-B1 or Myc-cyclin-B1/P300 shows enhancing lysine-33 acetylation reduces cyclin-B1 binding.

the positive charge of catalytic lysine-33 in CDK1 is essential for cyclin-B binding and its loss either by acetylation or a mutation to glutamine abrogates the interaction.

Electrostatic tethering of catalytic lysine-33 dictates surface interactions between CDK1 and cyclin-B

Next, we investigated the mechanistic underpinnings of lysine-33-dependent association of CDK1 and cyclin-B proteins. Examining the structure of ternary WT CDK1:cyclin-B:ATP complex revealed that residues 40–60 of CDK1 interface directly with cyclin-B. Specifically, in addition to the PSTAIRE-helix (residues 45–58), which has been previously described [5,17], we found that the random coil segment (residues 40–44) in CDK1 also interacts with cyclin-B, as implicated in CDK2:cyclin-A [5]. Importantly, the random coil segment is contiguous with the N-lobe-β3 (residue 28–36), containing lysine-33. It should be noted that combination mutants of residues in each of these segments in CDK1 have been shown to reduce cyclin-B binding [4]. However, the forces that orient these segments and help in stabilizing interactions between the proteins are still unknown.

These observations prompted us to investigate if the local electrostatic interactions of catalytic lysine-33 impinge on interface interactions of CDK1 with cyclin-B. Specifically, we carried out a statistical analysis of salt-bridge interactions in CDK1-WT, -K33Q and -K33Ac ternary complexes (Supplementary Table S2) during the initial (first 1 ns) stages of our 200-ns MD trajectory (Fig. 6c). We chose the 1-ns period of the trajectory since destabilization of the CDK1:cyclin-B interface, as assessed by inter-protein COM separations, occurred early in our MD production runs in CDK1-K33Q and -K33Ac systems. Our analysis clearly shows that the number of interfacial salt bridges is halved in the case of CDK1-K33Q and -K33Ac complexes, as compared to CDK1-WT, during the initial phase of our MD simulations (Fig. 6a), presaging the increase in inter-protein separations (Fig. 4e). Furthermore, we quantified the distributions of E_{NB} of interfacial salt bridge forming residues of CDK1 and cyclin-B (Supplementary table S2). Interestingly, we found the E_{NB} values to be significantly lower (by ~150–200 kcal/mol) and also highly variable when the charge state of lysine-33 is lost (Fig. 6b). Moreover, a more detailed analyses revealed that interfacial salt-bridge interactions involving both, acidic (D/E) and
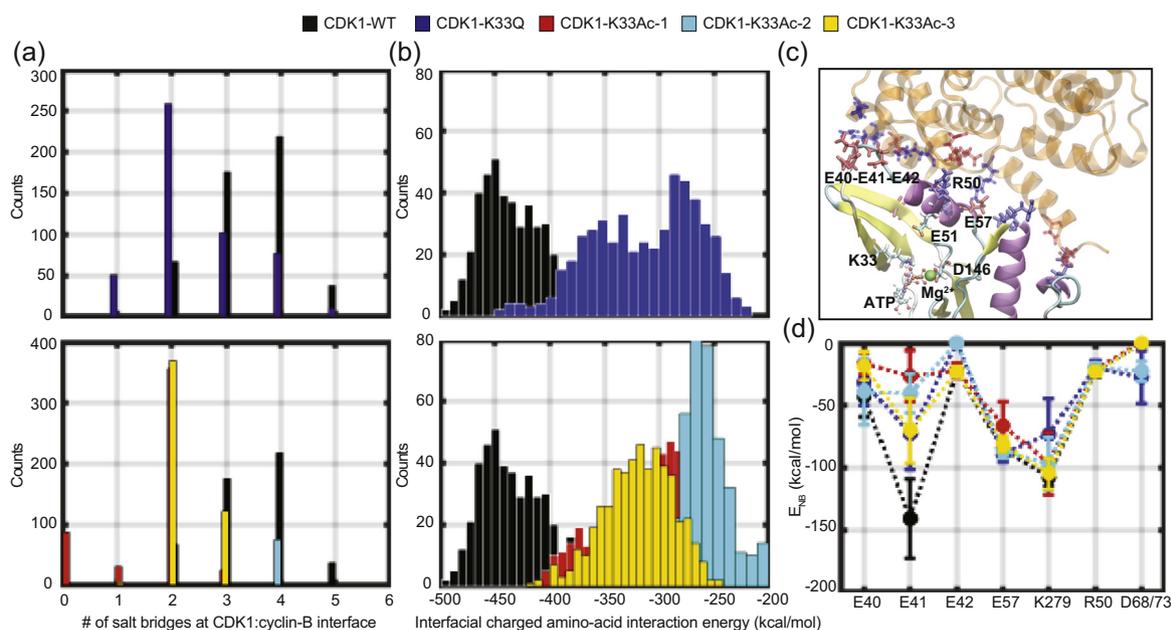
Fig. 6. Loss of CDK1 lysine-33 charge state affects surface electrostatic interactions with cyclin-B. (a) Reduction in the number of interfacial salt bridges between CDK1 and cyclin-B in CDK1:cyclin-B:ATP K33Q (top panel) and K33Ac systems (bottom panel) relative to WT. (b) Reduction in non-bonded interaction energies between acidic and basic residues at CDK1:cyclin-B interface in CDK1:cyclin-B:ATP K33Q (top panel) and K33Ac systems (bottom panel) relative to WT. (c) View of the CDK1:cyclin-B interface and its connectivity to the active site with catalytic triad residues (K33, D146, E51) and ATP. Key acidic and basic residues at the CDK1:cyclin-B interface are also shown. In this representation, we show only residues 30–148 and 250–280 in CDK1. (d) Comparison of non-bonded interaction energies (E_{NB}) of key acidic and basic residues of CDK1 with salt-bridge partner residues of cyclin-B shows maximum contribution by E41, which is dependent on K33 charge state. Error bars represent SD. The analysis is for data from the beginning of first 1 ns of NVT production runs for WT and mutant systems before CDK1–cyclin COM–COM separations increase for the latter.

basic (K/R) residues of CDK1 (Fig. S6a), as well as side-chain backbone salt bridges (Fig. S6b) were reduced in K33Q and K33Ac CDK1:cyclin-B:ATP complexes.

Our comprehensive analysis further demonstrated that, upon perturbing lysine-33, the largest changes in E_{NB} were observed for residue glutamate-41 (by ~100 kcal/mol) at the CDK1:cyclin-B interface (Fig. 6d). Interestingly, we found negligible perturbations in salt-bridge interactions formed by acidic and basic residues in the PSTAIRE-helix (arginine-50 and glutamate-57). Specifically, our results illustrate that the effects mediated by catalytic lysine-33 on glutamate-41 in the N-lobe-β3/C-helix linker loop of CDK1 may play a deterministic role in enabling CDK1:cyclin-B interactions. These findings are also illustrated in the form of movies (Supplementary Movies S1-S5).

Cdc2/CDK1 lysine-33 mutation blocks cell-cycle progression in *Schizosaccharomyces pombe*

To better understand physiological consequence of lysine-33 acetylation for CDK1 function, we turned to fission yeast, *S. pombe*, which shares the cell-cycle regulatory mechanisms with higher eukaryotes including humans [46,47] and is one of the best studied system for mitotic control. Indeed the first human CDK gene was cloned based on its ability to compliment a temperature-sensitive mutation in *cdc2* gene, *cdc2*-33 [46]. Unlike mammalian cells, the fission yeast cell cycle is controlled by a single CDK, Cdc2, which drives both G1/S and G2/M transitions, making it a simple model to study cell-cycle progression [48–50]. Moreover, a single CDK/cyclin pair (Cdc2p/Cdc13p) is sufficient to drive progression through the different phases of cell cycle [51].

We wanted to check if perturbing Sirtuin function in yeast would lead to any alteration in G2-M progression, possibly caused by hyperacetylation of Cdc2. Hence, we used *hst4* mutants, which has been associated with cell-cycle progression [52]. Furthermore, a previous report indicated that *hst4* mutants had elongated cells, similar to *cdc* mutants [52]. On scoring for mitotic entry and progression in the absence of *hst4*, we found that while mitotic entry seems to be marginally affected, there was a slight
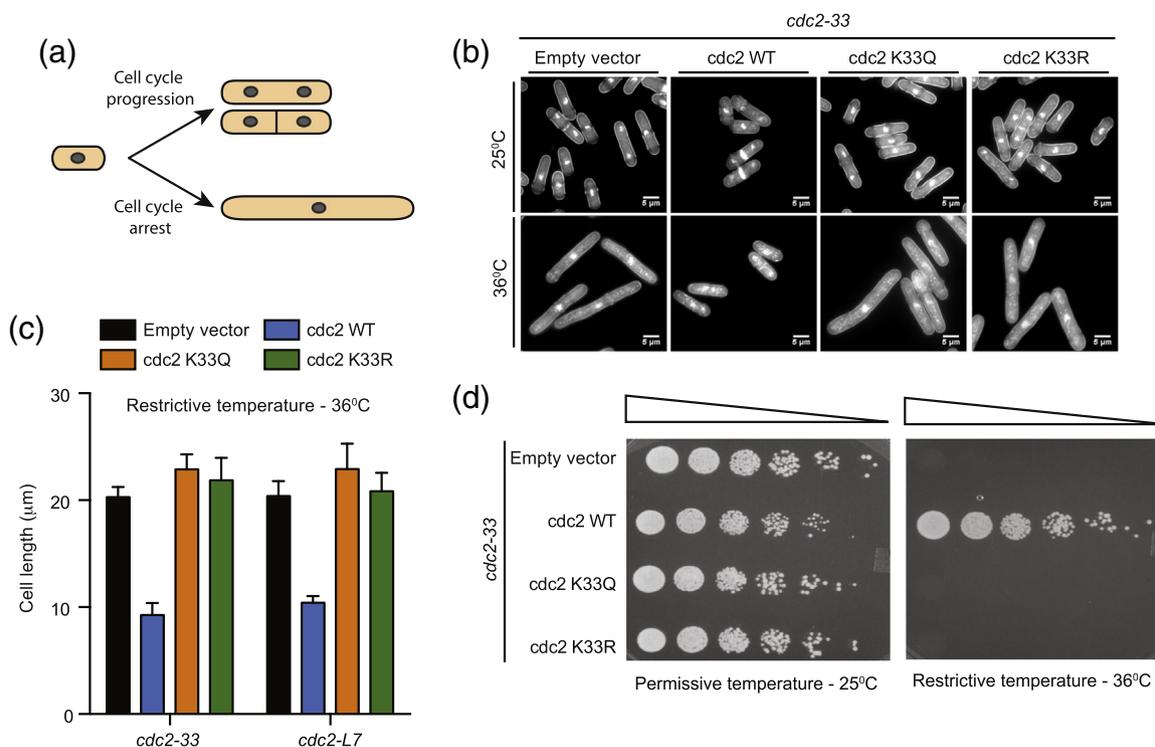
Fig. 7. Cdc2/CDK1 lysine-33 mutation blocks cell-cycle progression in *S. pombe* and fails to compliment *cdc2* ts mutants. (a) Schematic representation of cell length observed in fission yeast temperature-sensitive *cdc2* mutants at permissive temperature (normal cell-cycle progression) and restrictive temperature (cell-cycle arrest). (b) Representative images of DAPI and aniline blue co-stained cells of fixed samples after 16 h of induction, before (top panel) and after (bottom panel) shift at restrictive temperature for 4 h. Cells fixed after 4 h incubation at 36 °C. (c) Quantification of cell length measurements observed in *cdc2-33 and cdc2-L7* strains over-expressing indicated plasmids at restrictive temperature for 4 h. Measurement indicates mean cell length and SEM for three independent experiments where n = 500 for each sample. (d) Plate growth assay after 16 h of induction. Samples were 1:4 serially diluted, and plates were incubated at indicated temperature for 4–5 days.

but significant delay in progression through mitosis (Fig. S7a). These results are indeed interesting and could point toward a possible effect mediated by enhanced Cdc2 acetylation. However, loss of a deacetylase could impinge on several other factors, besides Cdc2, which might also be involved in G2-M progression, and further studies will likely provide novel insights into the role of Hst4 in mitotic progression. Thus, to check if the catalytic lysine in Cdc2 and its charge state indeed affected cell-cycle progression, we cloned *cdc2* K33Q and K33R mutants for further analyses.

Wild-type fission yeast cells grow to a length of about 14 μm before dividing. Temperature-sensitive (ts) *cdc2* mutants that undergo cell-cycle arrest at G2 and are unable to divide or form colonies, continue to grow when incubated at the restrictive temperature of 36 °C producing abnormally elongated cells with a single nucleus (Fig. 7a). Two independent ts alleles of *cdc2*, *cdc2-33* (A177T) and *cdc2-L7* (P208S), [48,53] arrest as elongated mononucleate cells when incubated at restrictive temperature of 36 °C (Fig. 7b and c and Fig. S7b–e), and fail to form viable colonies (Figs. 7d and S7f). Expressing wild-type *cdc2* gene under moderate-strength thiamine-repressible promoter (pnmt41) rescues the cell-cycle arrest in these mutants. These cells grow and divide at wild-type length distribution and are viable at the restrictive temperature of 36 °C (Fig. 7b–d and Fig. S7b–f). Unlike the cells rescued with Cdc2-WT, inducible expression of both Cdc2-K33Q and Cdc2-K33R failed to compliment the two *cdc2* ts mutants. These cells were elongated, arrested in G2 and also failed to form viable colonies (Fig. 7b–d and Fig. S7b–f). Although an earlier study in *Saccharomyces cerevisiae* had also shown that Cdc28-K40Q and Cdc28-K40R failed to complement *cdc28* null cells vis-à-vis viability [8], the effect on cell cycle was not addressed. Importantly, the findings described in the current study are consistent with our hypothesis about the significance of the catalytic lysine-33, which is evolutionarily conserved, in rendering CDK1/Cdc2 kinase competent, and hence its role in cell-cycle progression.

Discussion

Investigations into mechanisms that activate CDKs in general and CDK1 in particular are instrumental in our understanding of one of the most fundamental processes of eukaryotes, that is, cell division. In this study, we establish that the binding of cyclin-B to CDK1, which is essential for kinase activation, is allosterically regulated by the charge state of catalytic lysine-33 in CDK1. Besides providing mechanistic insights into structural changes, which impact cyclin-B binding upon acetylation, we demonstrate that a loss of positive charge on catalytic lysine-33 leads to cell-cycle arrest and lethality.

Our results establish catalytic lysine-33 as a molecular determinant of activity of CDK1. Mutating this lysine abolished CDK1 activity, which was independent of ATP binding and other regulatory inputs such as *via* Wee-1-mediated phosphorylation. In addition to pointing out a novel mechanism, these results also ruled out the possibility of gross structural perturbations that could have led to inactive CDK1 observed in the case of K33Q mutant. We would like to highlight that these are consistent with previous reports on CDK2, for example, which is very similar to CDK1.

Protein acetylation has been largely shown to occur on lysine residues and is now well established to act as a key regulatory modification [45,54,55]. In this context, our results show that the acetylation of CDK1 is negatively associated with cyclin-B binding and also that it is regulated in a cell cycle-dependent manner. Although acetyl mimic mutant of CDK1 was inactive, overexpression of CDK1-K33Q in the background of endogenous CDK1 did not lead to a dominant negative effect, unlike the phosphorylation defective mutants [31]. In our attempts to unravel the importance of the charge state of lysine-33, we discovered its importance in cyclin-B binding, which explains the lack of a dominant negative phenotype. Therefore, our results provide a novel mechanism for control of CDK1 activity and function.

With a few exceptions, almost all eukaryotic proteins kinases are known to possess a set of catalytic triad residues consisting of an N-lobe-β3 lysine, a C-helix glutamate and a DFG motif aspartate. Several reports, including most recent ones on PKA, have tried to dissect out both common and distinct mechanisms that render kinase competent conformations, which is dependent on the orientation of the catalytic triad residues [28]. It is important to note that uniquely in CDKs, binding of cyclins moves the C-helix containing catalytic glutamate, thereby bringing together the catalytic triad residues [5]. Hence, while cyclin binding is essential, whether this interaction is regulated and structural determinants that enable complexation are still unknown. In this context, using both biochemical and high-resolution computational analyses, we establish that the charge state of lysine-33 in CDK1, which is lost upon acetylation, plays a pivotal role in stabilizing intra-molecular tethers at the active site that are required for facilitating cyclin-B binding.

Although previous reports have shown that CDKs are acetylated and this inhibits their kinase activity, mechanistic insights are lacking [9–11,15,16]. In this context, we now show that the catalytic lysine in CDK1 exerts a dual control, orienting the ATP in the active-site pocket and allosterically facilitating cyclin-B binding. In addition, we have also addressed the importance of CDK1 acetylation or loss of the charge state of catalytic lysine on G2-M progression using the acetyl-mimic mutant of Cdc2/CDK1 in *S. pombe*. We note that CDK1 knockdown has been shown to

have variable effects on mammalian cells [56]. Therefore, using the yeast model not only eliminates possible compensatory roles of CDK2 [57] but also shows that the novel mechanism of acetylation-based regulation of cyclin binding uncovered here is evolutionarily conserved. As stated earlier and well established in the field, Cdc2 and CDK1 are highly conserved both at structural and functional levels [46]. Highlighting the physiological relevance of catalytic lysine and its charge state, we illustrate that mutating Cdc2 lysine-33 leads to cell-cycle arrest and reduces the viability in *S. pombe*.

In conclusion, our study highlights how local perturbations involving a key catalytic residue have long-range effects on protein–protein interactions. Importantly, our results suggest that acetylation of CDK1 prevents cyclin-B binding and therefore highlight deacetylation, which naturally unmasks the charge state of lysine-33, as a key determinant of CDK1:cyclin-B binding. Considering that other CDKs and EPKs are also acetylated at similar active-site lysines, impact of acetylation on binding to cognate partners or substrates remains to be uncovered.

Materials and Methods

Cell culture and transfection

HEK293T, HeLa-TetOn and mouse embryonic fibroblast cells were grown in DMEM high-glucose medium (Sigma-D777) supplemented with 10% fetal bovine serum (Gibco) or 10% newborn calf serum (Gibco) and 1% antibiotic–antimycotic solution (Gibco), and maintained under standard 5% CO_2 conditions. Cells were transfected using Lipofectamine 2000 (Life Technologies) or Fugene 6 (Roche) as per manufacturer's instructions. For inducible expression, 2 µg/ml doxycycline (Sigma) was added to the medium as indicated. For inhibiting HDACs or Sirtuins, cells were treated with 400 nM trichostatin A or 5 mM NAM, respectively, for 16 h. Sf21 (*Spodoptera frugiperda*) insect cells (Thermo Fisher) were grown in Graces' media containing antibiotic solution (Sigma) and 10% fetal bovine serum (Gibco) at 25 °C.

Yeast and bacterial culture

S. pombe strains were transformed with *pREP41* plasmid encoding wild-type or mutant *cdc2* gene using fast lithium acetate transformation method [58]. All strains were cultured in YE or EMM (MP Biomedicals) media with necessary supplements. Thiamine (10 µM) in EMM was used to suppress the *nmt41* promoter. For induction, cells initially cultured in EMM media containing thiamine were washed and subsequently cultured in EMM media without thiamine at 25 °C. After 16 h of induction, the cultures were shifted to restrictive temperature of 36 °C for 4 h. *Escherichia coli DH5α* cells were cultured in LB media supplemented with 100 µg/ml ampicillin for amplification of plasmids. Two percent agar was used for solid media.

Cell synchronization

Cells plated at 50% confluency were treated with 150 µM mimosine (Sigma) for 16 h to synchronize the cells in G1/S phase. To obtain cells synchronized in different phases, mimosine-treated cells were washed twice with PBS and released into fresh medium. Cells collected at 2–3, 5–6 and 7–8 h post-release corresponded to S-phase, G2-phase and G2/M-phase, respectively, as assessed by flow cytometry and phospho-H3 (S10) levels. To synchronize cells in G2 phase, 9 µM RO-3306 (Sigma) was used for 16 h, and for G2/M synchronization, cells were treated with Nocodazole (100 ng/ml) for 8 h after mimosine release.

FSBA labeling

CDK1-HA immunoprecipitates on beads were treated with 50 µM FSBA (Sigma) in 0.1% PBS–Triton-X-100 for 15 min at 30 °C with constant shaking, washed four times with 0.5% PBS–Triton-X-100 for 5 min at 4 °C on rotor and boiled in SDS gel loading buffer to elute the bound proteins. Western blotting was performed using α-FSBA antibodies and normalized to the amount of immunoprecipitated CDK1.

ATP binding and competition assays

The ATP binding assay was performed using the ATP affinity kit (Jena Bioscience) as per manufacturer's protocol. Briefly, the TNN cell lysate was dialyzed overnight at 4 °C against dialysis buffer (PBS, 1 mM EDTA, 1 mM DTT) with two buffer changes to remove the bound ATP-Mg^{2+}. The dialyzed lysate was diluted with the binding buffer containing protease inhibitor cocktail and incubated with equilibrated control or ATP beads for 2 h at 4 °C on rotor. For ATP competition, increasing amount of ATP was added in the dialyzed lysate before incubation with equilibrated control or ATP beads. The beads were washed thrice with the wash buffer for 15 min at 4 °C on rotor and boiled in SDS gel loading buffer to elute the bound proteins.

Modeling of CDK1:cyclin-B:ATP ternary complexes

Our computational modeling studies were initiated using a crystal structure of cyclin-B bound CDK1

(PDB ID: 4Y72) solved by Brown and co-workers [17]. Although an ATP-free CDK1:cyclin-B1 complex (PDB ID: 4YC3) was also available, we ascertained that the inhibitor-bound 4Y72 structure was a better starting model for our simulation studies as it presents a more catalytically competent active site [17]. Furthermore, the active-site catalytic triad conformations and the CDK–cyclin interface in 4Y72 are very similar (see Fig. S3a and b) to recently reported CDK1:cyclin-B1 crystal structures (PDB IDs: 6UG2, 6UG3, 6UG4) bound to other inhibitors with a wide range of K_d values (32–950 nM) [34]. The 4Y72 structure was bound to an inhibitor as well as the accessory protein CKS2, both of which were removed. The resultant structure lacked ATP and C-terminal residues (resid: 290–297) for CDK1. We modeled the missing C-terminal CDK1 residues (resid: 290–297) using the loop modeling module in Modeller version 9 [59]. An ATP molecule was then introduced in the active site of the CDK1:cyclin-B binary complex using the crystal structure of CDK2:cyclin-A:ATP ternary complex as a reference (PDB ID: 1FIN) to create a WT CDK1:cyclin-B:ATP ternary complex model. Specifically, we used the ATP coordinates from the 1FIN structure and inserted it at the active site of the CDK1:cyclin-B complex retaining the same interactions of ATP with the active-site aspartate-146 residue as in the 1FIN structure. After this step, we created two more mutant CDK1:cyclin-B:ATP complex models by replacing the lysine-33 in the WT model with either glutamine (K33Q) or acetyl lysine (K33Ac). For all three model complexes (WT, K33Q, K33Ac), hydrogen atoms were added using the psfgen utility in VMD [60]. Then the modeled complexes were immersed in a large rectangular water box (explicit solvent model) of dimension $126 \times 145 \times 128$ Å^3. The net charges of the model complexes were +3 for WT and +2 for K33Q/K33Ac. Therefore, 3 Cl$^-$ ions were added to WT and 2Cl$^-$ ions to K33Q/K33Ac solvent boxes to neutralize the systems.

Supplementary data to this article can be found online at https://doi.org/10.1016/j.jmb.2019.04.005.

CRediT authorship contribution statement

Shaunak Deota: Conceptualization, Data curation, Formal analysis, Investigation, Methodology, Validation, Visualization, Writing - original draft, Writing - review & editing. **Sivasudhan Rathnachalam:** Investigation, Methodology, Validation, Visualization. **Kanojia Namrata:** Investigation, Methodology, Validation, Visualization. **Mayank Boob:** Investigation, Methodology, Validation, Visualization. **Amit Fulzele:** Data curation, Formal analysis, Investigation, Methodology, Validation, Visualization, Writing - original draft. **Radhika. S.** Investigation, Methodology, Validation, Visualization. **Shubhra Ganguli:** Investigation, Methodology, Validation, Visualization. **Chinthapalli Balaji:** Investigation, Methodology, Validation, Visualization. **Stephanie Kaypee:** Investigation, Methodology, Validation, Visualization. **Krishna Kant Vishwakarma:** Investigation, Methodology, Validation, Visualization. **Tapas Kumar Kundu:** Supervision, Methodology. **Rashna Bhandari:** Supervision, Methodology. **Anne Gonzalez de Peredo:** Funding acquisition, Supervision, Investigation, Methodology, Visualization. **Mithilesh Mishra:** Conceptualization, Methodology, Visualization. **Ravindra Venkatramani:** Conceptualization, Data curation, Formal analysis, Funding acquisition, Investigation, Project administration, Supervision, Visualization, Writing - original draft, Writing - review & editing. **Ullas Kolthur-Seetharam:** Conceptualization, Data curation, Formal analysis, Funding acquisition, Investigation, Project administration, Supervision, Visualization, Writing - original draft, Writing - review & editing.

Acknowledgments

References

[1] D.O. Morgan, Cyclin-dependent kinases: engines, clocks, and microprocessors, Annu. Rev. Cell Dev. Biol. 13 (1997) 261–291.

[2] M. Malumbres, Cyclin-dependent kinases, Genome Biol. 15 (2014) 122.

[3] M.E. Crosby, Cell cycle: principles of control, Yale J. Biol. Med. 80 (2007) 141–142.

[4] B. Ducommun, P. Brambilla, M.A. Félix, B.R. Franza, E. Karsenti, G. Draetta, cdc2 phosphorylation is required for its interaction with cyclin, EMBO J. 10 (1991) 3311–3319.

[5] P.D. Jeffrey, A.A. Russo, K. Polyak, E. Gibbs, J. Hurwitz, J. Massague, et al., Mechanism of CDK activation revealed by the structure of a cyclinA–CDK2 complex, Nature. 376 (1995) 313–320.

[6] M.C. Morris, C. Gondeau, J.A. Tainer, G. Divita, Kinetic mechanism of activation of the Cdk2/cyclin A complex. Key role of the C-lobe of the Cdk, J. Biol. Chem. 277 (2002) 23847–23853.

[7] H.L. De Bondt, J. Rosenblatt, J. Jancarik, H.D. Jones, D.O. Morgan, S.H. Kim, Crystal structure of cyclin-dependent kinase 2, Nature. 363 (1993) 595–602.

[8] C. Choudhary, C. Kumar, F. Gnad, M.L. Nielsen, M. Rehman, T.C. Walther, et al., Lysine acetylation targets protein complexes and co-regulates major cellular functions, Science. 325 (2009) 834–840.

[9] A. Sabo, M. Lusic, A. Cereseto, M. Giacca, Acetylation of conserved lysines in the catalytic core of cyclin-dependent kinase 9 inhibits kinase activity and regulates transcription, Mol. Cell. Biol. 28 (2008) 2201–2212.

[10] F. Mateo, M. Vidal-Laliena, N. Canela, A. Zecchin, M. Martinez-Balbas, N. Agell, et al., The transcriptional co-activator PCAF regulates cdk2 activity, Nucleic Acids Res. 37 (2009) 7072–7084.

[11] J. Lee, N. Yun, C. Kim, M.Y. Song, K.S. Park, Y.J. Oh, Acetylation of cyclin-dependent kinase 5 is mediated by GCN5, Biochem. Biophys. Res. Commun. 447 (2014) 121–127.

[12] V.B. Pillai, N.R. Sundaresan, S.A. Samant, D. Wolfgeher, C.M. Trivedi, M.P. Gupta, Acetylation of a conserved lysine residue in the ATP binding pocket of p38 augments its kinase activity during hypertrophy of cardiomyocytes, Mol. Cell. Biol. 31 (2011) 2349–2363.

[13] M. Sarikhani, S. Mishra, P.A. Desingu, C. Kotyada, D. Wolfgeher, M.P. Gupta, et al., SIRT2 regulates oxidative stress-induced cell death through deacetylation of c-Jun NH, Cell Death Differ. 25 (9) (2018) 1638–1656.

[14] M. Sarikhani, S. Mishra, S. Maity, C. Kotyada, D. Wolfgeher, M.P. Gupta, et al., SIRT2 deacetylase regulates the activity of GSK3 isoforms independent of inhibitory phosphorylation, Elife. 7 (2018).

[15] H. Zhang, S.H. Park, B.G. Pantazides, O. Karpiuk, M.D. Warren, C.W. Hardy, et al., SIRT2 directs the replication stress response through CDK9 deacetylation, Proc. Natl. Acad. Sci. U. S. A. 110 (2013) 13546–13551.

[16] J. Lee, Y.U. Ko, Y. Chung, N. Yun, M. Kim, K. Kim, et al., The acetylation of cyclin-dependent kinase 5 at lysine 33 regulates kinase activity and neurite length in hippocampal neurons, Sci. Rep. 8 (2018), 13676.

[17] N.R. Brown, S. Korolchuk, M.P. Martin, W.A. Stanley, R. Moukhametzianov, M.E. Noble, et al., CDK1 structures reveal conserved and unique features of the essential cell cycle CDK, Nat. Commun. 6 (2015) 6769.

[18] D. Santamaria, C. Barriere, A. Cerqueira, S. Hunt, C. Tardy, K. Newton, et al., Cdk1 is sufficient to drive the mammalian cell cycle, Nature. 448 (2007) 811–815.

[19] S.A. Wang, C.Y. Hung, J.Y. Chuang, W.C. Chang, T.I. Hsu, J.J. Hung, Phosphorylation of p300 increases its protein degradation to enhance the lung cancer progression, Biochim. Biophys. Acta 1843 (2014) 1135–1149.

[20] T. Sasaki, B. Maier, K.D. Koclega, M. Chruszcz, W. Gluba, P.T. Stukenberg, et al., Phosphorylation regulates SIRT1 function, PLoS One 3 (2008) e4020.

[21] C. Norbury, J. Blow, P. Nurse, Regulatory phosphorylation of the p34cdc2 protein kinase in vertebrates, EMBO J. 10 (1991) 3321–3329.

[22] D. Leroy, C. Birck, P. Brambilla, J.P. Samama, B. Ducommun, Characterisation of human cdc2 lysine 33 mutations expressed in the fission yeast *Schizosaccharomyces pombe*, FEBS Lett. 379 (1996) 217–221.

[23] M. Hannink, D.J. Donoghue, Lysine residue 121 in the proposed ATP-binding site of the v-mos protein is required for transformation, Proc. Natl. Acad. Sci. U. S. A. 82 (1985) 7894–7898.

[24] M.P. Kamps, B.M. Sefton, Neither arginine nor histidine can carry out the function of lysine-295 in the ATP-binding site of p60src, Mol. Cell. Biol. 6 (1986) 751–757.

[25] G. Weinmaster, M.J. Zoller, T. Pawson, A lysine in the ATP-binding site of P130gag-fps is essential for protein-tyrosine kinase activity, EMBO J. 5 (1986) 69–76.

[26] Y. Ebina, E. Araki, M. Taira, F. Shimada, M. Mori, C.S. Craik, et al., Replacement of lysine residue 1030 in the putative ATP-binding region of the insulin receptor abolishes insulin- and antibody-stimulated glucose uptake and receptor kinase activity, Proc. Natl. Acad. Sci. U. S. A. 84 (1987) 704–708.

[27] G.H. Iyer, M.J. Moore, S.S. Taylor, Consequences of lysine 72 mutation on the phosphorylation and activation state of cAMP-dependent kinase, J. Biol. Chem. 280 (2005) 8800–8807.

[28] H.S. Meharena, X. Fan, L.G. Ahuja, M.M. Keshwani, C.L. McClendon, A.M. Chen, et al., Decoding the interactions regulating the active state mechanics of eukaryotic protein kinases, PLoS Biol. 14 (2016), e2000127.

[29] K.L. Gould, P. Nurse, Tyrosine phosphorylation of the fission yeast cdc2+ protein kinase regulates entry into mitosis, Nature. 342 (1989) 39–45.

[30] K.L. Gould, S. Moreno, D.J. Owen, S. Sazer, P. Nurse, Phosphorylation at Thr167 is required for *Schizosaccharomyces pombe* p34cdc2 function, EMBO J. 10 (1991) 3297–3309.

[31] W. Krek, E.A. Nigg, Mutations of p34cdc2 phosphorylation sites induce premature mitotic events in HeLa cells: evidence for a double block to p34cdc2 kinase activation in vertebrates, EMBO J. 10 (1991) 3331–3341.

[32] G.J. Den Haese, N. Walworth, A.M. Carr, K.L. Gould, The Wee1 protein kinase regulates T14 phosphorylation of fission yeast Cdc2, Mol. Biol. Cell 6 (1995) 371–385.

[33] S. van den Heuvel, E. Harlow, Distinct roles for cyclin-dependent kinases in cell cycle control, Science. 262 (1993) 2050–2054.

[34] D.J. Wood, S. Korolchuk, N.J. Tatum, L.Z. Wang, J.A. Endicott, M.E.M. Noble, et al., Differences in the conformational energy landscape of CDK1 and CDK2 suggest a mechanism for achieving selective CDK inhibition, Cell Chem. Biol. 26 (2019) 121–130 (e5).

[35] S.S. Taylor, A.P. Kornev, Protein kinases: evolution of dynamic regulatory proteins, Trends Biochem. Sci. 36 (2011) 65–77.

[36] J.A. Endicott, M.E. Noble, L.N. Johnson, The structural basis for control of eukaryotic protein kinases, Annu. Rev. Biochem. 81 (2012) 587–613.

[37] R. Bayliss, A. Fry, T. Haq, S. Yeoh, On the molecular mechanisms of mitotic kinase activation, Open Biol. 2 (2012), 120136.

[38] E.S. Child, T. Hendrychová, K. McCague, A. Futreal, M. Otyepka, D.J. Mann, A cancer-derived mutation in the PSTAIRE helix of cyclin-dependent kinase 2 alters the stability of cyclin binding, Biochim. Biophys. Acta 1803 (2010) 858–864.

[39] S. Atherton-Fessler, L.L. Parker, R.L. Geahlen, H. Piwnica-Worms, Mechanisms of p34cdc2 regulation, Mol. Cell. Biol. 13 (1993) 1675–1685.

[40] M. Anostario Jr., M.L. Harrison, R.L. Geahlen, Immunochemical detection of adenine nucleotide-binding proteins with antibodies to 5′-p-fluorosulfonylbenzoyladenosine, Anal. Biochem. 190 (1990) 60–65.

[41] V. Mayya, K. Rezual, L. Wu, M.B. Fong, D.K. Han, Absolute quantification of multisite phosphorylation by selective reaction monitoring mass spectrometry: determination of inhibitory phosphorylation status of cyclin-dependent kinases, Mol. Cell. Proteomics 5 (2006) 1146–1157.

[42] K. Coulonval, H. Kooken, P.P. Roger, Coupling of T161 and T14 phosphorylations protects cyclin B-CDK1 from premature activation, Mol. Biol. Cell 22 (2011) 3971–3985.

[43] J. Baeza, J.A. Dowell, M.J. Smallegan, J. Fan, D. Amador-Noguez, Z. Khan, et al., Stoichiometry of site-specific lysine acetylation in an entire proteome, J. Biol. Chem. 289 (2014) 21326–21338.

[44] J. Gil, A. Ramírez-Torres, D. Chiappe, J. Luna-Peñaloza, F.C. Fernandez-Reyes, B. Arcos-Encarnación, et al., Lysine acetylation stoichiometry and proteomics analyses reveal pathways regulated by sirtuin 1 in human cells, J. Biol. Chem. 292 (2017) 18129–18144.

[45] C. Choudhary, B.T. Weinert, Y. Nishida, E. Verdin, M. Mann, The growing landscape of lysine acetylation links metabolism and cell signalling, Nat. Rev. Mol. Cell Biol. 15 (2014) 536–550.

[46] M.G. Lee, P. Nurse, Complementation used to clone a human homologue of the fission yeast cell cycle control gene cdc2, Nature. 327 (1987) 31–35.

[47] C. Norbury, P. Nurse, Animal cell cycles and their control, Annu. Rev. Biochem. 61 (1992) 441–470.

[48] P. Nurse, P. Thuriaux, K. Nasmyth, Genetic control of the cell division cycle in the fission yeast *Schizosaccharomyces pombe*, Mol. Gen. Genet. 146 (1976) 167–178.

[49] P. Nurse, Y. Bissett, Gene required in G1 for commitment to cell cycle and in G2 for control of mitosis in fission yeast, Nature. 292 (1981) 558–560.

[50] P. Nurse, Cell cycle control genes in yeast, Trends Genet. 1 (1985) 51–55.

[51] D. Coudreuse, P. Nurse, Driving the cell cycle with a minimal CDK control network, Nature. 468 (2010) 1074–1079.

[52] L.L. Freeman-Cook, J.M. Sherman, C.B. Brachmann, R.C. Allshire, J.D. Boeke, L. Pillus, The *Schizosaccharomyces pombe* hst4(+) gene is a SIR2 homologue with silencing and centromeric functions, Mol. Biol. Cell 10 (1999) 3171–3186.

[53] P.A. Fantes, Control of timing of cell cycle events in fission yeast by the wee 1+ gene, Nature. 302 (1983) 153–155.

[54] E. Verdin, M. Ott, 50 Years of protein acetylation: from gene regulation to epigenetics, metabolism and beyond, Nat. Rev. Mol. Cell Biol. 16 (2015) 258–264.

[55] I. Ali, R.J. Conrad, E. Verdin, M. Ott, Lysine acetylation goes global: from epigenetics to metabolism and therapeutics, Chem. Rev. 118 (2018) 1216–1252.

[56] D. Cai, V.M. Latham, X. Zhang, G.I. Shapiro, Combined depletion of cell cycle and transcriptional cyclin-dependent kinase activities induces apoptosis in cancer cells, Cancer Res. 66 (2006) 9270–9280.

[57] L. L'Italien, M. Tanudji, L. Russell, X.M. Schebye, Unmasking the redundancy between Cdk1 and Cdk2 at G2 phase in human cancer cell lines, Cell Cycle 5 (2006) 984–993.

[58] J.B. Keeney, J.D. Boeke, Efficient targeted integration at leu1-32 and ura4-294 in *Schizosaccharomyces pombe*, Genetics. 136 (1994) 849–856.

[59] A. Sali, T.L. Blundell, Comparative protein modelling by satisfaction of spatial restraints, J. Mol. Biol. 234 (1993) 779–815.

[60] W. Humphrey, A. Dalke, K. Schulten, VMD: visual molecular dynamics, J. Mol. Graph. 14 (1996) 33–38 (27-8).